Published in final edited form as:
*Mol Imaging Biol*. 2010 June ; 12(3): 316–324. doi:10.1007/s11307-009-0256-6.

# $^{64}$Cu-Labeled Affibody Molecules for Imaging of HER2 Expressing Tumors

**Zhen Cheng**[1], **Omayra Padilla De Jesus**[2], **Daniel J. Kramer**[2], **Abhijit De**[1], **Jack M. Webster**[2], **Olivier Gheysens**[1], **Jelena Levi**[1], **Mohammad Namavari**[1], **Sen Wang**[1], **Jinha Mark Park**[1], **Rong Zhang**[2], **Hongguang Liu**[1], **Brian Lee**[2], **Faisal A. Syud**[2], and **Sanjiv Sam Gambhir**[1]

[1]Molecular Imaging Program at Stanford (MIPS), Departments of Radiology and Bioengineering, Bio-X Program, Stanford University, California, CA, 94305-5344, USA

[2]General Electric Company, Global Research Center, Niskayuna, NY, 12309, USA

## Abstract

**Introduction—**The development of molecular probes based on novel engineered protein constructs is under active investigation due to the great potential of this generalizable strategy for imaging a variety of tumor targets.

**Discussion—**In this report, human epidermal growth factor receptor type 2 (HER2)-binding Affibody molecules were radiolabeled with $^{64}$Cu and their imaging ability was further evaluated in tumor mice models to understand the promise and limitations of such probes. The anti-HER2 Affibody molecules in monomeric ($Z_{HER2:477}$) and dimeric [$(Z_{HER2:477})_2$] forms were site specifically modified with the maleimide-functionalized chelator, 1,4,7,10-tetraazacyclododecane-1,4,7-tris(acetic acid)-10-acetate mono (*N*-ethylmaleimide amide) (Mal-DOTA). The resulting DOTA–Affibody conjugates were radiolabeled with $^{64}$Cu and evaluated in nude mice bearing subcutaneous SKOV3 tumors. Biodistribution experiments showed that tumor uptake values of $^{64}$Cu-DOTA-$Z_{HER2:477}$ and $^{64}$Cu-DOTA-$(Z_{HER2:477})_2$ were 6.12±1.44% and 1.46±0.50% ID/g, respectively, in nude mice ($n$=3 each) at 4 h postinjection. Moreover, $^{64}$Cu-labeled monomer exhibited significantly higher tumor/blood ratio than that of radiolabeled dimeric counterpart at all time points examined in this study. MicroPET imaging of $^{64}$Cu-DOTA-$Z_{HER2:477}$ in SKOV3 tumor mice clearly showed good and specific tumor localization. This study demonstrates that $^{64}$Cu-labeled $Z_{HER2:477}$ is a promising targeted molecular probe for imaging HER2 receptor expression in living mice. Further work is needed to improve the excretion properties, hence dosimetry and imaging efficacy, of the radiometal-based probe.

### Keywords

Affibody; HER2; PET; Imaging; $^{64}$Cu



Correspondence to: Zhen Cheng; zcheng@stanford.edu.

## Introduction

Small proteins as platforms for imaging probe development have attracted significant interest because of their favorable properties (ease of preparation, possible production by chemical synthesis, high affinity and specificity, rapid blood clearance, quick and good tumor accumulation). Most importantly, some of these protein scaffolds have shown great potential for recognizing a variety of biomarkers [1–5]. Among them, Affibody molecules have recently received significant attention. Affibody is an engineered small protein scaffold with 58-amino acid residues and a three-helix bundle structure, as derived from one of the IgG-binding domains of staphylococcal protein A [4]. Many Affibody binders against desired targets have been identified and selected using phage-display technology [4].

Human epidermal growth factor receptor type 2 (HER2) is a well-established tumor target overexpressed in a wide variety of cancers including breast, ovarian, lung, gastric, and oral cancers [6–8]. It has been demonstrated as a molecular target for therapeutic intervention, a prognostic indicator of patient survival, and as a predictive marker of response to antineoplastic therapy [6–8]. Numerous radionuclides including $^{18}$F [9–11], $^{99m}$Tc [12–15], $^{111}$In [16–19], $^{90}$Y [20], $^{177}$Lu [20, 21], $^{68}$Ga [22], $^{125}$I [14, 23–25], $^{76/77/82}$Br [26], and $^{211}$At [27] have been used to label the anti-HER2 Affibody molecules for tumor imaging or radiotherapy. These studies have clearly demonstrated that Affibody molecules are a promising new class of cancer targeting ligands and worthy of further investigation for developing probes for different tumor targets.

Positron emission tomography (PET) imaging has high sensitivity, spatial resolution, and quantification ability, but with relatively higher cost. It is a great modality for imaging different molecular targets and events and is playing an important role in clinical cancer molecular imaging [28, 29]. Therefore, there is a potential demand to develop PET radioisotopes ($^{18}$F, $^{64}$Cu, $^{68}$Ga, etc.) labeled Affibody molecules for clinical applications. However, radiometal-labeled Affibody proteins have not been well investigated in the literature; only one abstract has reported to use $^{68}$Ga ($t_{1/2}$= 68 min)-labeled Affibody molecule for HER2 imaging to date [22]. Moreover, there is no study to systematically compare the *in vivo* performance of both monomeric and dimeric Affibodies using the same Affibody clone. Therefore, in this study, the commercially available anti-HER2 Affibody molecules in monomeric ($Z_{HER2:477}$) and dimeric [$(Z_{HER2:477})_2$] forms [23] were site specifically modified at the C terminus cysteine residue with the maleimide-functionalized chelator, 1,4,7,10-tetraazacyclododecane-1,4,7-β max tris (acetic acid)-10-acetate mono (*N*-ethylmaleimide amide) (Mal-DOTA; compound **3** in Fig. 1). The resulting DOTA–Affibody bioconjugates were then radiolabeled with the positron emitter $^{64}$Cu ($t_{1/2}$ =12.7 h, $E^{+}_{\beta}\max = 656\,keV$, 19%). The biological properties of the molecular probes were evaluated in nude mice bearing subcutaneous HER2 expression SKOV3 tumors. Subsequently, the ability of $^{64}$Cu-labeled HER2-binding Affibody proteins to image HER2 expression in living mice was also evaluated using small animal PET.

## Materials and Methods

### General Aspects

The anti-HER2 imaging agent Affibody molecule $Z_{HER2:477}$ and a bivalent Affibody protein anti-HER2 unconjugated $(Z_{HER2:477})_2$ (V D N K F N K E M R N A Y W E I A L L P N L N V A Q K R A F I R SLYDDPSQSANLLAEAKKLNDAQAPKC [21], purity >95% as provided by the vendor) were purchased from Affibody AB (Bromma, Sweden) and used directly for the chemical modification. 1,4,7,10-Tetraazacyclododecane-1,4,7,-tris(*t*-butylacetate)-1-succinimidyl acetate PF6 salt (or DOTA-mono-NHS-tris(tBu)ester) was purchased from Macrocyclics Inc. (Dallas, TX, USA). Dichloromethane, 2-(*tert*-butoxycarbonylaminooxy)acetic acid, triethylamine, *N*-(2-amino-ethyl)maleimide-trifluoroacetic acid (TFA) salt, *N*-hydroxybenzotriazole hydrate (HOBT), 1-ethyl-3-[3-dimethylaminopropyl] carbodiimide (EDC), *N*-hydroxysuccinimide (NHS), ethyl acetate, dithiothreitol (DTT), tricine, and 4-fluorobenzaldehyde were purchased from Sigma-Aldrich Chemical Co. (St. Louis, MO, USA). Dimethyl sulfoxide (DMSO) and ethyl acetate were purchased from Fisher Scientific (Pittsburgh, PA, USA). All other standard synthesis reagents were purchased from Sigma-Aldrich Chemical Co. (St. Louis, MO, USA). All chemicals were used without further purification. $^{64}Cu$ was provided by the Department of Medical Physics, University of Wisconsin at Madison (Madison, WI, USA).

A CRC-15R PET dose calibrator (Capintec Inc., Ramsey, NJ, USA) was used for all radioactivity measurements. Reversed-phase high-performance liquid chromatography (RP-HPLC) was performed on a Dionex Summit HPLC system (Dionex Corporation, Sunnyvale, CA, USA) equipped with a 170U 4-Channel UV–Vis absorbance detector and radioactivity detector (Carroll & Ramsey Associates, model 105S, Berkeley, CA, USA). UV detection wavelengths were 218, 254, and 280 nm for all the experiments. Analytical RP-HPLC columns (Vydac, Hesperia, CA, USA, 218TP510-C18, 10×250 mm) was used for analysis of labeled proteins. The mobile phase was solvent A, 0.1% TFA/$H_2O$, and solvent B, 0.1%TFA/acetonitrile. Matrix-assisted laser desorption/ionization time-of-flight mass spectrometry (MALDI-TOF-MS; model: Perseptive Voyager-DE RP Biospectrometer; Framingham, MA, USA) or an electrospray ionization time-of-flight mass spectrometer (ESI-TOF-MS; model: JMS-T100LC; JEOL, Tokyo, Japan) was performed by the Mass Spectrometry Lab at GE Global Research (Niskayuna, NY, USA). Human ovarian cancer SKOV3 and MDA-MB-435 melanoma cell lines were obtained from the American Type Tissue Culture Collection (Manassas, VA, USA). Female athymic nude mice (*nu/nu*) were purchased from Charles River Laboratories (Boston, MA, USA).

### Synthesis of Bifunctional Chelator Mal-DOTA

To a solution of DOTA-mono-NHS-tris(tBu)ester (200 mg, 0.248 mmol), triethylamine (70μL, 0.5 mmol) and *N*-(2-aminoethyl) maleimide TFA salt (42 mg, 0.165 mmol) in anhydrous dichloromethane (2 mL) were added. After stirring at room temperature overnight, the reaction mixture was partitioned between ethyl acetate (25 mL) and water (25 mL). The aqueous layer was separated and extracted with ethyl acetate (3×25 mL). The combined organic layers were washed with water (25 mL) and brine (25 mL), dried over anhydrous magnesium sulfate, and filtered. The filtrate was concentrated and purified by

column chromatography using 2% dichloromethane in methanol as the eluent to give the product Mal-DOTA tri-butyl ester (33 mg, 29% of theory, compound **2** in Fig. 1). Subsequently, to a solution of Mal-DOTA tri-butyl ester (18.4 mg, 0.0265 mmol) in anhydrous dichloromethane (0.2 mL), triisopropylsilane (25μL, mmol) and TFA (0.8 mL) were added. The reaction mixture was stirred at room temperature overnight and the solvent was removed under vacuum to give the product **3** in quantitative yield (17 mg).

### Synthesis of Affibody–Chelator Bioconjugates [DOTA-$Z_{HER2:477}$ and DOTA-$(Z_{HER2:477})_2$]

The Affibody molecule [$Z_{HER2:477}$ or $(Z_{HER2:477})_2$] was dissolved with freshly degassed phosphate buffer (pH7.4) at a concentration of 1 mg/mL. The disulfide linkage in the Affibody was reduced by the addition of DTT to a 20-mM concentration. The reaction mixture was incubated for 2 h and eluted through a NAP-5 column (GE Healthcare, Piscataway, NJ, USA) to remove excess of DTT reagent. The column had been previously equilibrated with degassed phosphate buffer, which was the same buffer used for elution of the Affibody. The reduced Affibody was collected and the bifunctional chelator, Mal-DOTA, was added (5–20 equivalents per equivalent of the Affibody) as a solution in DMSO. After mixing with vortex for 2 h, the reaction mixture was dialyzed overnight using Slide-A-Lyzer cassette of molecular weight (MW) cutoff (MWCO) 3.5 kDa (Pierce Biotechnology, Rockford, IL, USA) and MilliQ water as exchange solvent. The dialyzed sample was concentrated using Microcon or Amicon Ultra centrifuge filters MWCO 5 kDa (Millipore, Billerica, MA, USA). Characterization of the bioconjugated products was confirmed using MALDI-TOF-MS or liquid chromatography–ESI-MS (LC–ESI-MS). The purities of the bioconjugates were confirmed by HPLC.

### In Vitro Biacore Analysis of Affibody Bioconjugates

Binding interactions between the bioconjugates [DOTA-$Z_{HER2:477}$ and DOTA-$(Z_{HER2:477})_2$] and HER2/neu antigen were measured *in vitro* using surface plasmon resonance (SPR) detection on a Biacore™ 3000 instrument (GE Healthcare, Piscataway, NJ, USA). The extracellular domain of the HER2/neu antigen was obtained as a conjugate with the Fc region of human IgG (Fc-Her2) from R&D Systems (Minneapolis, MN, USA) and covalently attached to a CM-5 dextran-functionalized sensor chip (GE Healthcare, Piscataway, NJ, USA) pre-equilibrated with HBS-EP buffer (0.01 M 4-(2-hydroxyethyl)-1-piperazineethanesulfonic acid, pH7.4, 0.15 M NaCl, 3 mM ethylenediaminetetraacetic acid, 0.005% *v*/*v* surfactant P20) at 10μL/min and subsequently activated with EDC and NHS. The Fc-HER2 (5μg/mL) in 10 mM sodium acetate (pH5.5) was injected onto the activated sensor chip until the desired immobilization level (~3,000 resonance units) was achieved (2 min). Residual activated groups on the sensor chip were blocked by injection of ethanolamine (1 M, pH8.5). Any noncovalently bound conjugates were removed by repeated (5×) washing with 2.5 M NaCl and 50 mM NaOH. A second flow cell on the same sensor chip was treated identically, except with no Fc-HER2 immobilization, in order to serve as a control surface for refractive index changes and nonspecific binding interactions with the sensor chip. Prior to the kinetic study, binding of the target analyte was tested on both surfaces and a surface stability experiment was performed to ensure adequate removal of the bound analyte and regeneration of the sensor chip following treatment with 2.5 M NaCl and 50 mM NaOH. SPR sensorgrams were analyzed using the BIA evaluation software (GE

Healthcare, Piscataway, NJ, USA). The robustness of the kinetic model was determined by evaluation of the residuals and standard error for each of the calculated kinetic parameters, the "goodness of the fit" ($\chi^2$<10), and a direct comparison of the modeled sensorgrams to the experimental data. SPR measurements were collected at eight analyte concentrations (0–100 nM peptide) and the resulting sensorgrams were fitted to the Langmuir binding model.

### $^{64}$Cu Radiolabeling

The Affibody conjugate [DOTA-$Z_{HER2:477}$ or DOTA-$(Z_{HER2:477})_2$] was radiolabeled with $^{64}$Cu by addition of 185 MBq (5 mCi) of $^{64}CuCl_2$ [1μg DOTA-$(Z_{HER2:477})_2$ per 14.8 MBq $^{64}$Cu or 1μg DOTA-$Z_{HER2:477}$ per 7.4 MBq $^{64}$Cu] in 0.1 N NaOAc (pH5.5) buffer followed by a 1-h incubation at 40°C. The radiolabeled complex was then purified by a PD-10 column (GE Healthcare, Piscataway, NJ, USA). The product was washed out by phosphate buffered saline (PBS) and passed through a 0.22-μm Millipore filter into a sterile vial for *in vitro* and animal experiments. Radioanalytical HPLC was used to analyze the purified $^{64}$Cu-labeled Affibody molecules.

### Octanol/Water Partition Coefficient

To determine the lipophilicity of $^{64}$Cu-DOTA-$Z_{HER2:477}$ and $^{64}$Cu-DOTA-$(Z_{HER2:477})_2$, approximately 370 kBq of $^{64}$Cu-labeled complex in 500μL of PBS (pH7.4), was added to 500μL of octanol in an Eppendorf microcentrifuge tube. The resulting biphasic system was mixed vigorously for 10 min and left at room temperature for another 60 min. The two phases were then separated by centrifugation at 2,000×*g* for 5 min (model 5415R Eppendorf microcentrifuge; Brinkman, Westbury, NY, USA). From each layer, an aliquot of 100μL was removed and counted in a γ-counter (Packard Instruments). The partition coefficient (log *P*) was then calculated as a ratio of counts in the octanol fraction to the counts in the water fraction. The experiment was repeated three times.

### Cell Culture

SKOV3 cells were cultured in RPMI-1640 medium supplemented with 10% fetal bovine serum (FBS) and 1% penicillin–streptomycin (Invitrogen Life Technologies, Carlsbad, CA, USA). MDA-MB-435 cells were cultured in Leibovitz's L-15 medium with 2 mM L-glutamine supplemented with 0.01 mg/mL insulin, 10% FBS, and 1% penicillin–streptomycin in a sealed flask. All the cell lines were maintained in a humidified atmosphere of 5% $CO_2$ at 37°C, with the medium changed every other day. A confluent monolayer was detached with trypsin and dissociated into a single cell suspension for further cell culture.

### HER2 Western Analysis of Tumor Cells and Tissues

Expression of HER2 was verified in SKOV3 and MDA-MB-435 cells and tumor samples. Cells were harvested, washed twice with ice-cold PBS once, and lysed in 1× passive cell lysis buffer (Cell signaling, Danvers, MA, USA) for 10 min on ice. Estimated equal amount of the lysates were loaded in 7.5% Tris-HCl ReadyGel (BioRad, Hercules, CA, USA) and transferred onto nitrocellulose membrane (GE Healthcare, Piscataway, NJ, USA) with a semidry blotting system. The blots were probed with rabbit anti-HER2 antibody (Invitrogen, Carlsbad, CA, USA). The α-tubulin antibody was used as a loading control. Xenografted

SKOV3 and MDA-MB-435 tumors were harvested and immediately frozen in dry ice. Sodium dodecyl sulfate (SDS) lysis buffer (50 mM Tris, pH7.4, 2% SDS) containing Complete Mini protease inhibitor (Roche, Palo Alto, CA, USA) was used to lyse the tumors. After freezing at −80° C and thawing at 37°C three times, tumor lysates were centrifuged, and supernatant was used for protein detection as described above.

## Biodistribution Studies

All animal studies were carried out in compliance with Federal and local institutional rules for the conduct of animal experimentation. Approximately $1\times10^6$ SKOV3 cells suspended in Matrigel (BD Biosciences, San Jose, CA, USA) were implanted subcutaneously in the flanks of nude mice. Tumors were grown to a size of 500 to 750 mg (2–3 weeks), and the tumor bearing mice were subject to *in vivo* biodistribution and imaging studies. For some mice, the mice were first inoculated with $5\times10^6$ MDA-MB-435 cells. Two to 4 weeks postinoculation, these mice were inoculated with SKOV3 tumor on the other side of the flank.

For biodistribution studies, the SKOV3 tumor-bearing mice ($n$=3 for each group) were injected with radiolabeled Affibody proteins [$^{64}$Cu-DOTA-$Z_{HER2:477}$ (13–25μCi, 0.481–0.925 MBq, 0.12–0.23μg) and $^{64}$Cu-DOTA-$(Z_{HER2:477})_2$ (5–10μCi, 0.185–0.37 MBq, 0.02–0.04μg)] via the tail vein and sacrificed at different time points from 30 min to 20 h postinjection (p.i.). Tumor and normal tissues of interest were removed and weighed, and their radioactivity along with $^{64}$Cu standards of the injected dose was measured in a gamma-counter. The radioactivity uptake in the tumor and normal tissues was expressed as a percentage of the injected radioactive dose per gram of tissue (% ID/g).

## MicroPET Imaging

PET imaging of tumor-bearing mice was performed on a microPET R4 rodent model scanner (Siemens Medical Solutions USA, Inc., Knoxville, TN, USA). The mice bearing SKOV3 and MDA-MB-435 were injected with $^{64}$Cu-DOTA-$Z_{HER2:477}$ (70–85 μCi, 2.59–3.14 MBq, 0.65–0.79 μg) or $^{64}$Cu-DOTA-$(Z_{HER2:477})_2$ (100–120 μCi, 3.70–4.44 MBq, 0.48–0.56μg) via tail vein. For another group of mice bearing SKOV3 tumor only ($n$=6), three mice were treated with 300μg Herceptin, while another three were treated with PBS via tail vein injection. Forty-eight hours later, $^{64}$Cu-DOTA-$Z_{HER2:477}$ (70–85 μCi, 2.59–3.14 MBq, 0.65–0.79μg) was administrated to the both treated/control tumor mice. At different time p.i., the mice were anesthetized with 2% isoflurane and placed in the prone position and near the center of the field of view of microPET. The 5-min static scans were obtained and the images were reconstructed by a two-dimensional ordered subsets expectation maximum algorithm. The quantification analysis of PET images was then performed using the same method as previously reported [9].

## Statistical Methods

Statistical analysis was performed using the Student's $t$ test for unpaired data. A 95% confidence level was chosen to determine the significance between groups, with $P<0.05$ being significantly different.

# Results

## Chemistry

The maleimide amine linker was used to react with the tri-butyl protected mono-NHS DOTA chelator (compound **1**; Fig. 1) under conventional EDC/HOBT activation to form an amide. For the preparation of the compound **3**, the carboxylate version of DOTA was also tried using EDC/HOBT coupling but only starting material was recovered. The desired product (compound **2**) was obtained in a 29% yield and verified by ESI-MS and NMR. The measured molecular weight was consistent with the expected MW: *m/z*=695.52 for $[M+H]^+$ ($C_{34}H_{59}N_6O_9$, calculated MW= 695.86) and $^1$H-NMR (400 MHz, $CD_2Cl_2$): δ 1.49 (s, 18H), 1.51 (s, 9H), 2–2.4 (m, 8H), 2.5–3 (m, 14H), 3.2–3.6 (m, 6H), 6.76 (s, 2H). After the amine coupling, the tri-butyl groups in compound **2** were then cleaved under acidic condition. The deprotection reaction was clean, yielding the compound **3** quantitatively with no need for further purification. Compound **3** was verified by ESI-MS and NMR: *m/z*=527.29 for $[M+H]^+$ ($C_{22}H_{34}N_6O_9$, calculated MW=527.54) and $^1$H-NMR (400 MHz, DMSO): δ 3–4.2 (m, 28H), 7.05 (s, 2H).

The Mal-DOTA linker was then conjugated to the Affibody molecules. The use of 5–20 molar equivalents Mal-DOTA was enough to achieve quantitative coupling yields in 2 h. Moreover, the use of larger excess (200 equivalents) only gave the monosubstituted product, confirming that only the cysteine presenting in the Affibody proteins reacted selectively with the linker. MS analysis of the final products confirmed the absence of unreacted Affibodies and the presence of only the expected products. The MWs for the bioconjugates DOTA-$Z_{HER2:477}$ and DOTA-$(Z_{HER2:477})_2$ obtained were 7,277.50 and 14,563.81 with 25% and 47% recovery yields after purification, respectively (calculated MW=7,278.52 and 14,565.42 for **4** and **5**, respectively).

## Radiochemistry

DOTA conjugated $Z_{HER2:477}$ and $(Z_{HER2:477})_2$ were successfully labeled with $^{64}$Cu at 40°C for 1 h incubation. The purification of radiolabeling solution using a PD-10 column afforded $^{64}$Cu-DOTA-$(Z_{HER2:477})_2$ and $^{64}$Cu-DOTA-$Z_{HER2:477}$ with >95% radiochemical purity with modest specific activity [214μCi/μg (115.3 MBq/nmol) and 108μCi/μg (29.1 MBq/nmol), respectively]. HPLC analysis of $^{64}$Cu-labeled DOTA-$(Z_{HER2:477})_2$ and DOTA-$Z_{HER2:477}$ both showed one single peak with close retention time [21.6 and 24.0 min for $^{64}$Cu-DOTA-$(Z_{HER2:477})_2$ and $^{64}$Cu-DOTA-$Z_{HER2:477}$, respectively]. From the octanol–water partition coefficient measurements, the log *P* value of $^{64}$Cu-DOTA-$(Z_{HER2:477})_2$ and $^{64}$Cu-DOTA-$Z_{HER2:477}$ were determined to be −0.46±0.04 and 0.018±0.006, respectively, indicating intermediate hydrophilicity of both radiolabeled proteins.

## HER2 Binding Affinity of Affibody Bioconjugates

The results of Biacore binding studies of Affibody bio-conjugates are shown in Fig. 2. The binding affinities of DOTA-$(Z_{HER2:477})_2$ and DOTA-$Z_{HER2:477}$ were 100 pM and 1.5 nM, respectively (Fig. 2a, b). The binding affinities of these constructs still remain in a very promising range. The on rates for both DOTA conjugated molecules were very fast, with association constants in the range of $10^5$. In addition, the off rates were very slow, with

dissociation constants in the range of $10^{-4}$–$10^{-5}$, close to the sensitivity limits of the Biacore assay.

## HER2 Western Analysis of Tumor Cells and Tissues

The radiolabeled Affibody molecules were then evaluated in the SKOV3 ovarian cancer and MDA-MB-435 melanoma with different HER2 expression. Western blot analysis of HER2 expression in these two cultured tumor cell lines or xenografted tumor samples was performed and the results are shown in Fig. 3. Obviously, SKOV3 showed good HER2 expression in both cultured cells and tumor samples, while MDA-MB-435 cells and tumor exhibited minimum HER2 expression. Quantification analysis of western gel further revealed that HER2 expression in SKOV3 tumor tissue was 10–15-folds higher than that of MDA-MB-435 tumor.

## Biodistribution Studies

Biodistribution data for $^{64}$Cu-labeled DOTA-$(Z_{HER2:477})_2$ and DOTA-$Z_{HER2:477}$ at 1, 4, and 20 h are summarized in Table 1. $^{64}$Cu-DOTA-$Z_{HER2:477}$ exhibited much higher tumor uptake than that of $^{64}$Cu-DOTA-$(Z_{HER2:477})_2$ at all times ($P$<0.05). Rapid and moderate activity accumulation in the SKOV3 tumors was also observed for $^{64}$Cu-DOTA-$Z_{HER2:477}$ at early time point (3.86±0.58% ID/g at 1 h p.i.). Tumor uptake increased to 6.12±1.44% ID/g at 4 h, then the activity was slowly washed out from the tumor, and uptake was dropped to 3.65±0.69% ID/g over 20 h. Both $^{64}$Cu-DOTA-$Z_{HER2:477}$ and $^{64}$Cu-DOTA-$(Z_{HER2:477})_2$ displayed rapid blood clearance, with 0.75±0.22% and 2.27±0.27% ID/g blood uptake at 1 h, respectively. Extremely high renal uptake and retention were found for $^{64}$Cu-DOTA-$Z_{HER2:477}$ and $^{64}$Cu-DOTA-$(Z_{HER2:477})_2$. Moreover, $^{64}$Cu-DOTA-$Z_{HER2:477}$ showed about 1–1.5-fold higher renal uptake than $^{64}$Cu-DOTA-$(Z_{HER2:477})_2$. Relatively high liver uptake was also observed for $^{64}$Cu-labeled Affibody bioconjugates. But at 1 h p.i., $^{64}$Cu-labeled Affibody proteins show much higher uptake (% ID/organ) in kidney than that of liver and intestines (data not shown). These data confirmed that $^{64}$Cu-labeled proteins were mainly cleared via the urinary system. Finally, it was observed that both $^{64}$Cu-DOTA-$Z_{HER2:477}$ and $^{64}$Cu-DOTA-$(Z_{HER2:477})_2$ displayed relatively low uptake in all other normal organs.

## MicroPET Imaging

Decay-corrected coronal microPET images of a mouse bearing SKOV3 and MDA-MB-435 tumor at 1, 4, and 20 h after tail vein injection of $^{64}$Cu-DOTA-$Z_{HER2:477}$ or $^{64}$Cu-DOTA-$(Z_{HER2:477})_2$ are shown in Fig. 4a and b, respectively. For $^{64}$Cu-DOTA-$(Z_{HER2:477})_2$, SKOV3 tumor was visible but with moderate tumor-to-background contrast. However, MDA-MB-435 tumor showed very poor uptake and hence low tumor-to-background contrast. For $^{64}$Cu-DOTA-$Z_{HER2:477}$, SKOV3 tumor was clearly visualized with good tumor-to-background contrast at 1 to 20 h p.i. Low uptake in MDA-MB-435 tumor was also observed, making it very difficult to visualize the tumor. High activity accumulation was also observed in the kidney for both tracers, which was consistent with the finding from the biodistribution study.

In order to understand the relationship between the $^{64}$Cu-DOTA-$Z_{HER2:477}$ Affibody and a well-accepted HER2-targeting agent, Herceptin, and potentially specificity of the Affibody for HER2, mice bearing SKOV3 tumor ($n$=3) were first treated with 300μg of Herceptin or PBS via tail vein injection. At 48 h, the treated/control tumor mice were injected with $^{64}$Cu-DOTA-$Z_{HER2:477}$ and then imaged using microPET (Fig. 4c, d for control and treated animal, respectively). Pretreatment of SKOV3 tumor mice with HER2 binding protein (Herceptin) specifically reduced the uptake of $^{64}$Cu-DOTA-$Z_{HER2:477}$ in the tumor at 1, 3.5, and 24 h, resulting in a lower tumor to background ratios (Fig. 4d). MicroPET image region of interest quantification analysis was further performed and results are shown in Fig. 5. It was found that $^{64}$Cu-labeled monomer showed significantly higher tumor uptake than that of the dimer at 1, 4, and 20 h p.i. ($P$<0.05, $n$=3), while their muscle uptakes are similar. Overall, the PET imaging data agreed well with biodistribution results.

## Discussion

Affibody proteins, dimeric $(Z_{HER2:477})_2$ and monomeric $Z_{HER2:477}$, were selected for $^{64}$Cu radiolabeling because Affibody has been demonstrated to be a promising platform for developing probes to a variety of targets [3, 4]. By taking advantage of well-established maleimide–sulfhydryl chemistry [16], the maleimide-functionalized chelator, Mal-DOTA, was prepared in good yield and site specifically conjugated to the C terminus cysteine residue of $(Z_{HER2:477})_2$ and $Z_{HER2:477}$. Therefore, the Affibody proteins can be labeled with radiometals. The radiolabeling strategy described here is the same as the one reported previously [16]. Chelator Mal-DOTA was used in both studies for site-specific conjugation with the thiol group in the cysteine that is at the C terminus of Affibody. However, different clones of Affibodies were used in these two studies. Monomeric and dimeric $Z_{HER2:477}$ which are commercially available were used in this study, while $Z_{HER2:342}$ and H6-$Z_{HER2:342}$ were used in the literature [16]. Other nonsite-specific radiolabeling methods have also been reported [18, 23], where the lysine groups in the Affibody were used for radiolabeling. However, these approaches may generate heterogeneous products with reduced capacity because of the multiple lysine residues present in the Affibody including some which are responsible for receptor recognition. To the contrary, the site-specific conjugation of Mal-DOTA provides a pure homogenous product. Biacore analysis of the binding affinities of Affibody bioconjugates reveals that DOTA conjugated $(Z_{HER2:477})_2$ and $Z_{HER2:477}$ preserve high binding affinities to HER2 (in pico- and low nanomolar range). Because $(Z_{HER2:477})_2$ and $Z_{HER2:477}$ are large molecules and the binding residues are far away from the C terminus, it would be expected that modification of the C terminus cysteine with a relatively small metal chelator would be unlikely to interfere with the binding of the proteins.

$^{64}$Cu-labeled dimer and monomer exhibit rapid tumor accumulation and blood clearance, which are the major advantages of using these relatively small synthetic proteins as imaging agents compared to large long circulating proteins such as full antibodies. Furthermore, it was found that although DOTA-conjugated dimer exhibited higher HER2 binding affinity than that of monomer, $^{64}$Cu-labeled dimer showed much lower SKOV3 tumor accumulation and tumor-to-normal organ ratios than that of radiolabeled monomer. This finding is in

consistent with the *in vivo* distribution patterns of different clones of anti-HER2 Affibody proteins labeled with radioiodine [23, 30].

Obviously, $^{64}$Cu-labeled monomer could be used as a lead candidate for further HER2 imaging studies. This result clearly demonstrates that the binding affinity of a probe is not the only factor determining its tumor localization; other properties of the probe such as size, lipophilicity, and charge likely also play important roles for the probe's *in vivo* biological behavior. Many Affibody analogs with different properties (affinity, size, charge, and lipophilicity) are being synthesized in our laboratories and further evaluated in animal models, in order to understand what causes the difference. Relatively high liver uptake and moderate retention are also observed for the $^{64}$Cu-labeled dimer and monomer. The increased liver uptake over time is likely due to the release of uncoordinated $^{64}$Cu from radiolabeled protein by decomposition in the blood or transchelation in the liver [31]. Lastly, the $^{64}$Cu-labeled dimer exhibits better tumor retention that that of monomer. The tumor uptake of the dimer at 4 and 24 h p.i. maintain the same level (1.46% *vs* 1.53% ID/g, $P>0.05$), while a significant amount of activity for monomer is washed out from the tumor (6.12% *vs* 3.65% ID/g). This is likely caused by the lower binding affinity of monomer.

Very high kidney uptake and retention are observed for $^{64}$Cu-labeled Affibody molecules. The radiation dose to the kidney, a radiation-sensitive organ, may likely be a concern if the particularly high-energy $^{64}$Cu probe is used in clinic. Further optimization of the probe for achieving better tumor targeting and pharmacokinetic properties are under active investigation in our laboratories, in order to eventually move the Affibody-based probe into clinical HER2 imaging. Several strategies in the peptide/antibody-based imaging field may be applied to reduce the relatively high kidney uptake: (1) modification of the amino acid sequence of the Affibody to modulate the surface charge, lipophilicity, and binding affinity of the protein, which may also include PEGylation, (2) coinjection of cold amino acids such as lysine, which is an established method in the field of peptide based radioimaging/radiotherapy for reducing the kidney uptake, (3) use of cleavable linkers specific to mechanisms in the kidney, and (4) use of different radioisotopes such as radiohalogens, etc. Indeed, it is found that $^{18}$F-labeled Affibody molecules show much lower kidney uptake and retention [9, 11]. Furthermore, a recent study also demonstrates that the kidney uptake of $^{99m}$Tc-labeled Affibodies can be dramatically reduced by carefully selection of the amino acid chelators [32]. Overall, it is likely that kidney uptake and retention of the radiolabeled Affibodies could be minimized.

MicroPET imaging and quantification analysis of $^{64}$Cu-labeled $(Z_{HER2:477})_2$ and $Z_{HER2:477}$ in mice bearing SKOV3 and MDA-MB-435 tumor at 1, 4, and 20 h after tail vein injection reveal good SKOV3 tumor-to-background ratio for $^{64}$Cu-DOTA-$Z_{HER2:477}$, while $^{64}$Cu-DOTA-$(Z_{HER2:477})_2$ SKOV3 tumor-to-background ratio is low (Fig. 4a, b). The clear tumor PET imaging of $^{64}$Cu-DOTA-$Z_{HER2:477}$ at as early as 1 h p.i. apparently indicates the rapid tumor accumulation and fast normal organ clearance of monomeric Affibody molecule. Furthermore, both tracers display low uptake in the MDA-MB-435 tumor with low HER2 expression. These results are consistent with the findings obtained from the biodistribution studies. Moreover, the specificity of $^{64}$Cu-DOTA-$Z_{HER2:477}$ is demonstrated by the reduced SKOV3 tumor uptake in the mice which were pretreated with HER2 binding antibody,

Herceptin. This result does potentially vary from the published literature [17]. Possible reasons for our results include (1) different clones of anti-HER2 Affibody molecules used in these two studies and thus uncommon epitope between them, (2) steric hindrance from the Herceptin antibody, or (3) internalization of HER2 upon Herceptin binding and inaccessibility to the Affibody [33].

Overall, $^{64}$Cu-DOTA-$Z_{HER2:477}$ microPET imaging is a potential strategy for not only detection HER2-positive tumors but also differentiation tumors with different HER2 expression in living subjects. It is also noteworthy to point out that the anti-HER2 Affibody molecule $Z_{HER2:342}$ labeled with $^{68}$Ga and $^{111}$In have been used in imaging human breast cancer patients, indicating the low immunogenicity of this molecular probe derived from staphylococcal protein A [22].

## Conclusion

Site-specific $^{64}$Cu-labeled $Z_{HER2:477}$ and $(Z_{HER2:477})_2$ have been synthesized. Biodistribution and microPET imaging studies further demonstrate that $^{64}$Cu-labeled $Z_{HER2:477}$ is a promising molecular probe for imaging HER2 receptor expression in living mice. Strategies to further improve the labeling and biodistribution of the Affibody molecule and Affibody molecules against other targets are also under investigation. Affibody-based probes can likely be translated into multiple imaging and disease applications.

## Acknowledgments

This work was supported, in part, by National Cancer Institute (NCI) Small Animal Imaging Resource Program (SAIRP) grant R24 CA93862, NCI *In Vivo* Cellular Molecular Imaging Center (ICMIC) grant P50 CA114747 (SSG), and General Electric Global Research (SSG). We also thank Dr. Joshua Hoerner and Hans Grade of GE Global Research for their technical support and Dr. Alan Cuthbertson and Dr. Alex Gibson of GE Healthcare for their review of the manuscript.

## Abbreviations

| | |
|---|---|
| **DOTA** | 1,4,7,10-Tetraazacyclododecane-1,4,7,10-tetraacetic acid |
| **PET** | Positron emission tomography |
| **HPLC** | High-performance liquid chromatography |
| **p.i** | Postinjection |

## References

1. Nygren PA, Skerra A. Binding proteins from alternative scaffolds. J Immunol Methods. 2004; 290:3–28. [PubMed: 15261569]
2. Binz HK, Amstutz P, Pluckthun A. Engineering novel binding proteins from nonimmunoglobulin domains. Nat Biotechnol. 2005; 23:1257–1268. [PubMed: 16211069]
3. Binz HK, Pluckthun A. Engineered proteins as specific binding reagents. Curr Opin Biotechnol. 2005; 16:459–469. [PubMed: 16005204]
4. Nilsson FY, Tolmachev V. Affibody molecules: new protein domains for molecular imaging and targeted tumor therapy. Curr Opin Drug Discov Devel. 2007; 10:167–175.
5. Cortez-Retamozo V, Backmann N, Senter PD, et al. Efficient cancer therapy with a nanobody-based conjugate. Cancer Res. 2004; 64:2853–2857. [PubMed: 15087403]

6. Meric-Bernstam F, Hung MC. Advances in targeting human epidermal growth factor receptor-2 signaling for cancer therapy. Clin Cancer Res. 2006; 12:6326–6330. [PubMed: 17085641]
7. Robert NJ, Favret AM. HER2-positive advanced breast cancer. Hematol Oncol Clin North Am. 2007; 21:293–302. [PubMed: 17512450]
8. Ferretti G, Felici A, Papaldo P, Fabi A, Cognetti F. HER2/neu role in breast cancer: from a prognostic foe to a predictive friend. Curr Opin Obstet Gynecol. 2007; 19:56–62. [PubMed: 17218853]
9. Cheng Z, De Jesus OP, Namavari M, et al. Small-animal PET imaging of human epidermal growth factor receptor type 2 expression with site-specific $^{18}$F-labeled protein scaffold molecules. J Nucl Med. 2008; 49:804–813. [PubMed: 18413392]
10. Namavari M, Padilla De Jesus O, Cheng Z, et al. Direct site-specific radiolabeling of an Affibody protein with 4-[$^{18}$F]fluorobenzaldehyde via oxime chemistry. Mol Imaging Biol. 2008; 10:177–181. [PubMed: 18481153]
11. Kramer-Marek G, Kiesewetter DO, Martiniova L, Jagoda E, Lee SB, Capala J. [$^{18}$F]FBEM-$Z_{(HER2:342)}$-Affibody molecule—a new molecular tracer for *in vivo* monitoring of HER2 expression by positron emission tomography. Eur J Nucl Med Mol Imaging. 2008; 35:1008–1018. [PubMed: 18157531]
12. Tran T, Engfeldt T, Orlova A, et al. *In vivo* evaluation of cysteine-based chelators for attachment of $^{99m}$Tc to tumor-targeting affibody molecules. Bioconjug Chem. 2007; 18:549–558. [PubMed: 17330952]
13. Engfeldt T, Orlova A, Tran T, et al. Imaging of HER2-expressing tumours using a synthetic Affibody molecule containing the $^{99m}$Tc-chelating mercaptoacetyl-glycyl-glycyl-glycyl ($MAG_3$) sequence. Eur J Nucl Med Mol Imaging. 2007; 34:722–733. [PubMed: 17146656]
14. Orlova A, Nilsson FY, Wikman M, et al. Comparative *in vivo* evaluation of technetium and iodine labels on an anti-HER2 affibody for single-photon imaging of HER2 expression in tumors. J Nucl Med. 2006; 47:512–519. [PubMed: 16513621]
15. Engfeldt T, Tran T, Orlova A, et al. $^{(99m)}$Tc-chelator engineering to improve tumour targeting properties of a HER2-specific Affibody molecule. Eur J Nucl Med Mol Imaging. 2007; 18:1956–1964.
16. Ahlgren S, Orlova A, Rosik D, et al. Evaluation of maleimide derivative of DOTA for site-specific labeling of recombinant affibody molecules. Bioconjug Chem. 2008; 9:235–243. [PubMed: 18163536]
17. Orlova A, Tolmachev V, Pehrson R, et al. Synthetic affibody molecules: a novel class of affinity ligands for molecular imaging of HER2-expressing malignant tumors. Cancer Res. 2007; 67:2178–2186. [PubMed: 17332348]
18. Tolmachev V, Nilsson FY, Widstrom C, et al. $^{111}$In-benzyl-DTPA-$Z_{HER2:342}$, an affibody-based conjugate for *in vivo* imaging of HER2 expression in malignant tumors. J Nucl Med. 2006; 47:846–853. [PubMed: 16644755]
19. Orlova A, Rosik D, Sandstrom M, Lundqvist H, Einarsson L, Tolmachev V. Evaluation of [$^{(111/114m)}$In]CHX-A″-DTPA-Z ($HER_{2:342}$), an Affibody ligand conjugate for targeting of HER2-expressing malignant tumors. Q J Nucl Med Mol Imaging. 2007; 51:1–10. [PubMed: 17372566]
20. Fortin MA, Orlova A, Malmstrom PU, Tolmachev V. Labelling chemistry and characterization of [$^{90}$Y/$^{177}$Lu]-DOTA-$Z_{HER2:342–3}$ Affibody molecule, a candidate agent for locoregional treatment of urinary bladder carcinoma. Int J Mol Med. 2007; 19:285–291. [PubMed: 17203203]
21. Tolmachev V, Orlova A, Pehrson R, et al. Radionuclide therapy of HER2-positive microxenografts using a $^{177}$Lu-labeled HER2-specific Affibody molecule. Cancer Res. 2007; 67:2773–2782. [PubMed: 17363599]
22. Baum R, Orlova A, Tolmachev V, Feldwisch J. Receptor PET/CT and SPECT using an Affibody molecule for targeting and molecular imaging of HER2 positive cancer in animal xenografts and human breast cancer patients. J Nucl Med. 2006; 47(Suppl):108P.
23. Orlova A, Magnusson M, Eriksson TL, et al. Tumor imaging using a picomolar affinity HER2 binding affibody molecule. Cancer Res. 2006; 66:4339–4348. [PubMed: 16618759]

24. Steffen AC, Orlova A, Wikman M, et al. Affibody-mediated tumour targeting of HER-2 expressing xenografts in mice. Eur J Nucl Med Mol Imaging. 2006; 33:631–638. [PubMed: 16538504]
25. Steffen AC, Wikman M, Tolmachev V, et al. *In vitro* characterization of a bivalent anti-HER-2 affibody with potential for radionuclide-based diagnostics. Cancer Biother Radiopharm. 2005; 20:239–248. [PubMed: 15989469]
26. Mume E, Orlova A, Larsson B, et al. Evaluation of ((4-hydroxyphenyl)ethyl)maleimide for site-specific radiobromination of anti-HER2 affibody. Bioconjug Chem. 2005; 16:1547–1555. [PubMed: 16287254]
27. Steffen AC, Almqvist Y, Chyan MK, et al. Biodistribution of $^{211}$At labeled HER-2 binding affibody molecules in mice. Oncol Rep. 2007; 17:1141–1147. [PubMed: 17390057]
28. Gambhir SS. Molecular imaging of cancer with positron emission tomography. Nat Rev Cancer. 2002; 2:683–693. [PubMed: 12209157]
29. Massoud TF, Gambhir SS. Molecular imaging in living subjects: seeing fundamental biological processes in a new light. Genes Dev. 2003; 17:545–580. [PubMed: 12629038]
30. Tolmachev V, Mume E, Sjöberg S, Frejd FY, Orlova A. Influence of valency and labelling chemistry on *in vivo* targeting using radioiodinated HER2-binding Affibody molecules. Eur J Nucl Med Mol Imaging. 2009; 36:692–701. [PubMed: 19066886]
31. Boswell CA, Sun X, Niu W, et al. Comparative *in vivo* stability of copper-64-labeled cross-bridged and conventional tetraazamacrocyclic complexes. J Med Chem. 2004; 47:1465–1474. [PubMed: 14998334]
32. Ekblad T, Tran T, Orlova A, et al. Development and preclinical characterisation of $^{99m}$Tc-labelled Affibody molecules with reduced renal uptake. Eur J Nucl Med Mol Imaging. 2008; 35:2245–2255. [PubMed: 18594815]
33. Ekerljung L, Steffen AC, Carlsson J, Lennartsson J. Effects of HER2-binding affibody molecules on intracellular signaling pathways. Tumour Biol. 2006; 27:201–210. [PubMed: 16651854]

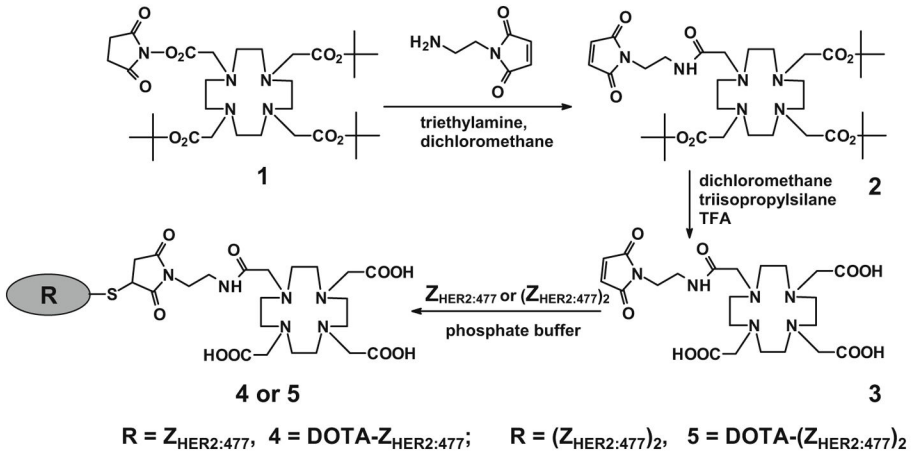


**Fig. 1.**

Synthetic schemes for bifunctional chelator Mal-DOTA preparation and conjugation of the chelator to the anti-HER2 Affibody molecules [$Z_{HER2:477}$ and $(Z_{HER2:477})_2$].

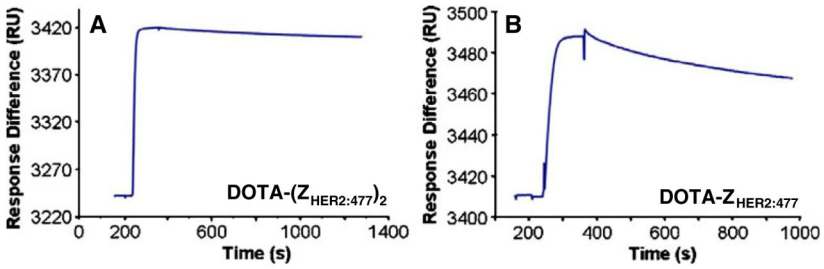


**Fig. 2.**

Biosensor binding studies of Affibody bioconjugates [DOTA-$(Z_{HER2:477})_2$ (**a**) and DOTA-$Z_{HER2:477}$ (**b**)]. Sensorgrams were obtained after injection of the purified Affibody molecules over a sensor chip flow-cell surface containing amine-coupled Fc-HER2 chimeric protein.

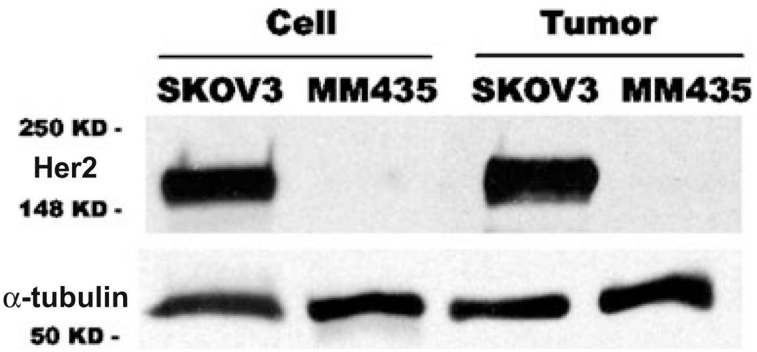


**Fig. 3.**

Western blot analysis of HER2 expression in SKOV3 ovarian cancer and MDA-MB-435 (abbreviated as MM435) melanoma in cultured tumor cells (labeled as *Cell*) and xenografted tumor samples (labeled as *Tumor*). Much higher level of HER2 is found in SKOV3 than that of in MDA-MB-435 for both cultured cells and tumor samples.

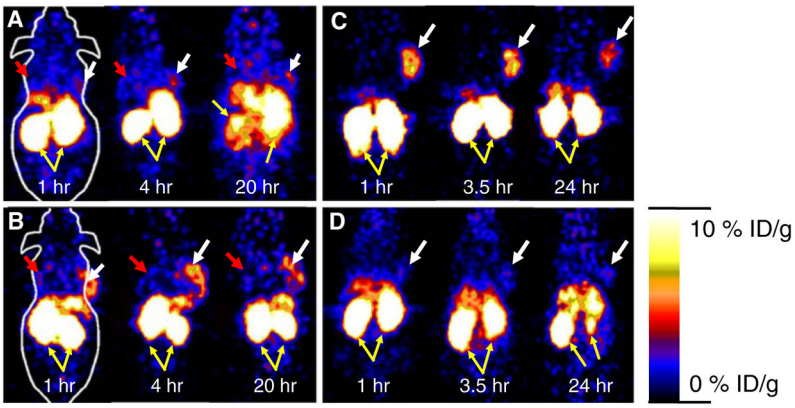


**Fig. 4.**

Decay corrected coronal microPET images of *nu*/*nu* mice bearing SKOV3 (indicated by *white arrows*) and MDA-MB-435 tumor (indicated by *red arrows*) at 1, 4, and 20 h after tail vein injection of $^{64}$Cu-DOTA-$(Z_{HER2:477})_2$ (**a**) and $^{64}$Cu-DOTA-$Z_{HER2:477}$ (**b**). Decay corrected coronal microPET images of SKOV3 bearing mice which were pretreated with PBS (**c**) or 300μg of Herceptin (**d**) 48 h before probe administration at 1, 3.5, and 24 h after tail vein injection of $^{64}$Cu-DOTA-$Z_{HER2:477}$. *Yellow arrows* indicate location of kidneys.

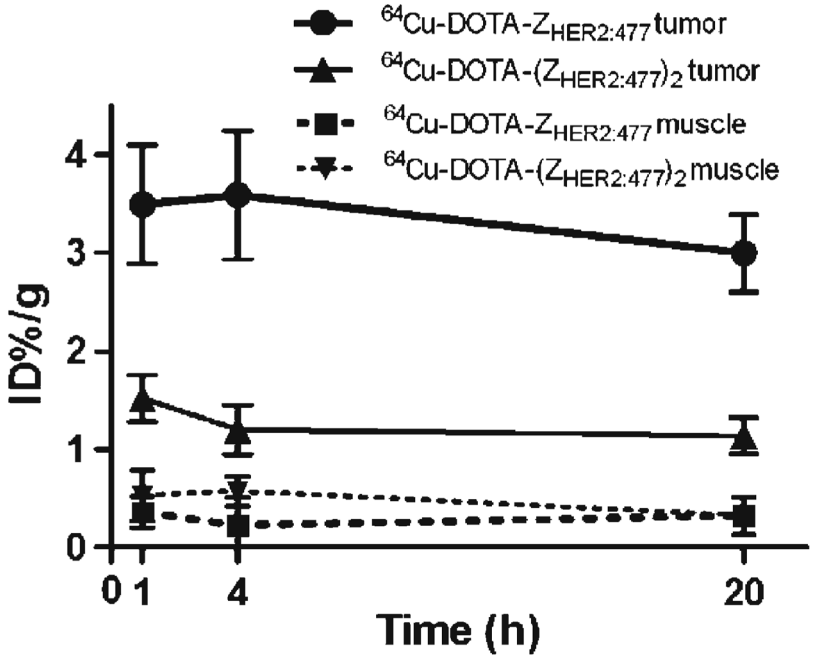


**Fig. 5.**

Tumor and muscle—time activity curves derived from the multitime point microPET imaging of mice bearing SKOV3 tumor. The regions of interests are shown as mean % ID/g ± SD (*n*=3).

**Table 1**

Biodistribution data for $^{64}$Cu-DOTA-$Z_{HER2:477}$ and $^{64}$Cu-DOTA-$(Z_{HER2:477})_2$ in nude mice bearing subcutaneously xenotransplanted SKOV3 human ovarian cancer

| Organ (% ID/g) | 1 h | | 4 h | | 20 h | |
|---|---|---|---|---|---|---|
| | DOTA-$Z_{HER2}$ | DOTA-$(Z_{HER2})_2$ | DOTA-$Z_{HER2}$ | DOTA-$(Z_{HER2})_2$ | DOTA-$Z_{HER2}$ | DOTA-$(Z_{HER2})_2$ |
| Tumor | 3.86±0.58 | 2.01±0.46 | 6.12±1.44 | 1.46±0.50 | 3.65±0.69 | 1.53±0.35 |
| Blood | 0.75±0.22 | 2.27±0.27 | 0.52±0.22 | 0.73±0.01 | 0.71±0.02 | 0.74±0.18 |
| Heart | 0.99±0.24 | 1.51±0.21 | 1.08±0.50 | 1.07±0.16 | 1.87±0.22 | 1.69±0.34 |
| Liver | 5.24±0.82 | 11.61±1.92 | 7.06±1.68 | 12.24±3.75 | 10.41±1.26 | 11.32±2.27 |
| Lungs | 2.92±0.60 | 3.14±1.42 | 2.13±0.26 | 1.73±0.40 | 3.74±0.74 | 2.56±0.52 |
| Muscle | 0.76±0.14 | 0.59±0.07 | 0.66±0.14 | 0.37±0.01 | 0.51±0.12 | 0.35±0.02 |
| Kidney | 206.26±22.36 | 114.33±11.22 | 237.51±34.49 | 75.21±5.74 | 129.69±14.43 | 37.95±5.55 |
| Spleen | 1.43±0.13 | 2.80±0.13 | 1.76±0.77 | 2.09±0.77 | 1.83±0.17 | 2.04±1.36 |
| Brain | 0.11±0.01 | 0.17±0.08 | 0.15±0.06 | 0.08±0.01 | 0.24±0.04 | 0.15±0.04 |
| Intestine | 2.45±0.10 | 1.81±0.49 | 1.84±0.88 | 2.14±0.28 | 3.22±0.72 | 2.14±0.33 |
| Skin | 1.01±0.25 | 1.63±0.23 | 0.88±0.26 | 1.06±0.41 | 1.23±0.12 | 1.15±0.38 |
| Stomach | 1.77±0.07 | 0.51±0.26 | 2.67±1.37 | 1.39±0.16 | 3.46±0.70 | 0.90±0.15 |
| Pancreas | 0.56±0.08 | 0.50±0.34 | 0.56±0.20 | 0.84±0.24 | 0.99±0.12 | 0.84±0.17 |
| Bone | 0.29±0.13 | 0.84±0.08 | 0.35±0.07 | 0.73±0.09 | 0.53±0.23 | 0.79±0.12 |
| Ratios | | | | | | |
| T/Blood | 5.28±0.91 | 0.91±0.33 | 12.44±3.39 | 2.00±0.69 | 5.12±0.87 | 2.06±0.04 |
| T/Muscle | 5.29±1.61 | 3.44±0.66 | 9.47±2.46 | 3.96±1.43 | 7.23±0.39 | 4.43±1.02 |

Data are expressed as the percentage administered activity (injected dose) per gram of tissue±standard deviation after intravenous injection of 370 kBq (10 μCi) tracers at 1, 4, and 20 h (*n*=3)

*T* tumor, *DOTA-Z*$_{HER2}$ $^{64}$Cu-DOTA-$Z_{HER2:477}$, *DOTA-(Z*$_{HER2}$*)2* $^{64}$Cu-DOTA-$(Z_{HER2:477})_2$